British Journal of Pharmacology

DOI:10.1111/bph.12437
www.brjpharmacol.org

RESEARCH PAPER

Molecular analysis of ATP-sensitive K^+ channel subunits expressed in mouse vas deferens myocytes

Kazuomi Iwasa[1], Hai-Lei Zhu[2], Atsushi Shibata[3], Yoshihiko Maehara[1] and Noriyoshi Teramoto[2]

[1]*Department of Surgery and Science, Graduate School of Medical Sciences, Kyushu University, Fukuoka, Japan,* [2]*Department of Pharmacology, Faculty of Medicine, Saga University, Saga, Japan, and* [3]*Department of Bioorganic and Synthetic Chemistry, Graduate School of Pharmaceutical Sciences, Kyushu University, Fukuoka, Japan*

Correspondence
Noriyoshi Teramoto, Department of Pharmacology, Faculty of Medicine, Saga University, Saga 849-8501, Japan. E-mail: noritera@cc.saga-u.ac.jp

Keywords
K_{ATP} channels; $K_{IR}6.1$; SUR2B; vas deferens myocytes

Received
1 May 2013
Revised
10 September 2013
Accepted
13 September 2013

BACKGROUND AND PURPOSE

ATP-sensitive K^+ (K_{ATP}) channels, which are composed of $K_{IR}6.x$ associated with sulphonylurea receptor (SUR) subunits, have been detected in native smooth muscle cells, but it is currently not known which of these is expressed in mouse vas deferens myocytes.

EXPERIMENTAL APPROACH

Pharmacological and electrophysiological properties of K_{ATP} channels in mouse vas deferens myocytes were investigated using patch clamp techniques. Molecular biological analyses were performed to examine the properties of these K_{ATP} channels.

KEY RESULTS

During conventional whole-cell recording, pinacidil elicited an inward current that was suppressed by glibenclamide, a sulfonylurea agent, and by U-37883A, a selective $K_{IR}6.1$ blocker. When 0.3 mM ATP was added to the pipette solution, the peak amplitude of the pinacidil-induced current was much smaller than that recorded in its absence. When 3 mM UDP, GDP or ADP was included in the pipette solution, an inward current was elicited after establishment of the conventional whole-cell configuration, with potency order being UDP > GDP > ADP. These nucleoside diphosphate-induced inward currents were suppressed by glibenclamide. MCC-134, a SUR modulator, induced glibenclamide-sensitive K_{ATP} currents that were similar to those induced by 100 μM pinacidil. In the cell-attached configuration, pinacidil activated channels with a conductance similar to that of $K_{IR}6.1$. Reverse transcription PCR analysis revealed the expression of $K_{IR}6.1$ and SUR2B transcripts and immunohistochemical studies indicated the presence of $K_{IR}6.1$ and SUR2B proteins in the myocytes.

CONCLUSIONS AND IMPLICATIONS

Our results indicate that native K_{ATP} channels in mouse vas deferens myocytes are a heterocomplex of $K_{IR}6.1$ channels and SUR2B subunits.

Abbreviations

E_K, theoretical K^+ equilibrium potential; K_{ATP} channel, ATP-sensitive K^+ channel; K_{IR}, inwardly rectifying K^+ channel; MCC-134, N-methyl-1-[4-(1H-imidazol-1-yl)benzoyl]-N-methyl-cyclobutanecarbothioamide; NDP, nucleoside diphosphate; SUR, sulphonylurea receptor; Triton X, polyoxyethylene-p-isooctylphenol; U-37883A, 4-morpholinecarboximidine-N-1-adamantyl-N'-cyclohexylhydrochloride

Introduction

The vas deferens plays an important role in transporting sperm from the epididymis to the urethra as part of the male reproductive tract. The vas deferens receives a dense sympathetic innervation; it is well known that neurotransmission in the vas deferens is predominantly mediated by noradrenaline (NA) and ATP released from sympathetic nerves, which regulate smooth muscle contraction during ejaculation (Wassall *et al.*, 2009). In addition, the vas deferens also acts as a reservoir for sperm before ejaculation. Several important relaxant mechanisms of vas deferens smooth muscle have also been reported. For instance, elevating the cyclic GMP level, which subsequently activates PKG, causes a significant relaxation of rat vas deferens (Patel *et al.*, 1997). Similarly, Kato *et al.* (2000) reported that an increase in intracellular cyclic AMP inhibits NA-induced contractions by attenuating a nifedipine-insensitive Ca^{2+} influx. The mechanism of relaxation reported by Kato *et al.* (2000) was also independent of a reduction in intracellular concentrations of Ca^{2+} ($[Ca^{2+}]_i$) in guinea pig vas deferens. Furthermore, various types of ATP-sensitive K^+ channel (K_{ATP} channel) openers (including cromakalim and pinacidil) cause glibenclamide-sensitive muscle relaxation in both the rabbit (Eltze, 1989) and rat (Grana *et al.*, 1997) vasa deferentia, suggesting that K_{ATP} channels may be activated in vas deferens myocytes. In contrast, Harhun *et al.* (2003) recorded currents from voltage-gated K^+ channels in rat vas deferens using electrophysiological techniques, but concluded that the presence of voltage-independent K^+ channels (such as K_{ATP} channels and muscarine-activated K^+ channels) could not be detected. Thus, it is uncertain whether K_{ATP} channels are present in the vas deferens. Furthermore, K_{ATP} channel openers have been shown to reduce neurotransmitter release from sympathetic nerves, causing significant inhibition of stimulus-evoked smooth muscle contraction (Soares-da-Silva and Fernandes, 1990). Therefore, dispersed smooth muscle cells constitute an ideal model system in which to investigate the effects of K_{ATP} channel openers in the absence of sympathetic innervation.

During the last two decades, several types of K_{ATP} channel have been detected in native smooth muscle cells by the use of single-channel recordings, although the molecular properties of K_{ATP} channels have only been investigated using reverse transcription (RT)-PCR analytical methods (Teramoto, 2006). In the present experiments, we obtained the first electrophysiological, molecular and biochemical evidence for the subunit composition of K_{ATP} channels in single, freshly dispersed mouse vas deferens myocytes. The electrophysiological and pharmacological properties of K_{ATP} currents were investigated using conventional whole-cell recordings. Single-channel studies were carried out to determine the single-channel conductance of the native K_{ATP} channels. Furthermore, RT-PCR and immunohistochemical analyses were utilized to determine the transcript and protein expressions of K_{ATP} channel subunits (namely, the inwardly rectifying K^+ channel 6.x [$K_{IR}6.x$] family of pore-forming subunits, and the modulatory sulphonylurea receptor [SUR.x] subunits).

Methods

Cell dispersion

All animal experiments were approved by the animal care and use committee of the Faculty of Medicine, Saga University (Saga, Japan) and Graduate School of Medical Sciences, Kyushu University (Fukuoka, Japan). All studies involving animals are reported in accordance with the ARRIVE guidelines for reporting experiments involving animals (Kilkenny *et al.*, 2010; McGrath *et al.*, 2010). Male Balb/c mice (8–10 weeks of age) were killed by cervical dislocation. Vasa deferentia were removed and immediately placed in physiological salt solution (PSS, see below). Myocytes were freshly isolated by the gentle tapping method (Teramoto and Brading, 1996; Zhu *et al.*, 2008) and stored at 4°C. Relaxed spindle-shaped cells were used for patch clamp analysis within 3–4 h of isolation.

Electrophysiological recordings

Patch clamp experiments (conventional whole-cell configuration) were performed at room temperature (21–23°C), as described previously (Teramoto *et al.*, 2009). Glass pipettes of resistances between 3 and 5 MΩ were fabricated using a micropipette puller (P-97, Sutter Instruments, Navato, CA, USA). Junction potentials between the bath and pipette solutions were measured with a 3 M KCl reference electrode and were <1 mV; therefore, correction for these potentials was not made. The series resistance was compensated for at the beginning of each experiment. Single-channel recordings were also performed as previously described in symmetrical 140 mM K^+ conditions (Teramoto *et al.*, 2009). The capacitance noise was kept to a minimum by minimizing the level of the test solution in the recording electrode.

Data analysis

The data recording system used was similar to that described previously (Teramoto *et al.*, 2009). Whole-cell currents were low-pass filtered at 500 Hz (continuous traces) or 2 kHz (ramp currents) by an 8-pole Bessel filter, sampled at 25 ms (continuous traces) or 1 ms (ramp current) intervals, and analysed using a MacBook Pro computer (Apple Computer Japan, Tokyo, Japan) running Chart v5.5.6 software (ADInstruments Pty Ltd., Castle Hill, Australia). For single-channel recordings, the stored data were low-pass filtered at 2 kHz (-3 dB) and sampled with a digitization interval of 80 μs using 'PAT' software (kindly provided by Dr J. Dempster, University of Strathclyde, UK); events briefer than 80 μs were not included in the evaluation. The continuous traces displayed in the figures were obtained from records filtered at 1 kHz for presentation (digital sampling interval, 500 μs). Values for the channel open state probability (P_{open}) were measured at –70 mV, from 1 min recordings. Open probability was determined according to the equation:

$$NPo = \left(\sum_{j=1}^{N} t_j \cdot j \right) \Big/ T$$

where t_j is the time spent at each current level corresponding to $j = 0, 1, 2, \ldots N$, T is the duration of the recording, and N is the number of channels detected in the patch. Data points were fitted using a least-squares method.

Solutions and drugs

The following solutions were used to record K_{ATP} currents through K_{ATP} channels (Alexander *et al.*, 2013): PSS containing (in mM): 140 NaCl, 5 KCl, 1.2 $MgCl_2$, 2 $CaCl_2$, 5 glucose, 10 HEPES, titrated to pH 7.35–7.40 with Tris base; in some experiments, this was modified to make a 140 mM K^+ solution, by replacing 135 mM Na^+ with equimolar K^+; high K^+ pipette solution containing (in mM): 140 KCl, 5 glucose, 5 EGTA, 10 HEPES (Ph 7.35–7.40 with Tris). For single-channel recordings, symmetrical 140 mM K^+ conditions were used; the pipette and bath solutions contained respectively (in mM): 140 KCl, 1 $CaCl_2$, 1 $MgCl_2$, 5.5 glucose, 10 HEPES (pH 7.35–7.40 with Tris) and 140 KCl, 4.6 $MgCl_2$, 1 EGTA, 10 glucose, 10 HEPES (pH 7.35–7.40 with Tris). Cells were allowed to settle in the small experimental chamber (approximately 80 µL in volume) before perfusion with bath solution was initiated. The bath solution was superfused by gravity throughout the experiments at a rate of 2 mL·min^{-1}. Pinacidil, glibenclamide, MCC-134 (N-methyl-1-[4-(1H-imidazol-1-yl)benzoyl]-N-methyl-cyclobutanecarbothioamide) and U-37883A (4-morpholinecarboximidine-N-1-adamantyl-N′-cyclohexylhydrochloride) were prepared daily as 100 mM stock solutions in DMSO. The final concentration of DMSO was less than 0.3%, and did not affect potassium channels (Teramoto and Brading, 1996; Teramoto *et al.*, 2009). U-37883A, a selective $K_{IR}6.1$ blocker (Kovalev *et al.*, 2004), was purchased from Biomol Research Labs Inc. (Plymouth Meeting, PA, USA). MCC-134, a SUR modulator (Shindo *et al.*, 2000), was kindly provided by Tokyo Mitsubishi Pharmaceuticals (Tokyo, Japan). All other chemicals were purchased from Sigma-Aldrich (Sigma-Aldrich Japan K.K., Tokyo, Japan).

RNA preparation and RT-PCR analysis

Total RNA was extracted from dissociated isolated cells of mouse vas deferens, ventricle and cerebrum using Trizol Reagent (Invitrogen, Carlsbad, CA, USA). First-strand cDNA was synthesized from 1 µg of total RNA using the GeneAmp RNA PCR kit (Applied Biosystems, Foster City, CA, USA) with oligo dT primer, according to the manufacturer's instructions. The PCR reaction was performed using 1 µL of cDNA in 50 µL KOD plus (Toyobo Co. Ltd, Osaka, Japan) containing 0.3 µM of each primer. The cycling conditions for $K_{IR}6.x$ ($K_{IR}6.1$ and $K_{IR}6.2$) were 94°C for 2 min, followed by 35 cycles of 94°C for 15 s, 62°C for 30 s and 68°C for 30 s. The cycling conditions for SUR.x (SUR1 and SUR2A/B) were 94°C for 2 min, followed by 35 cycles of 94°C for 15 s, 66°C for 30 s and 68°C for 30 s. An aliquot of the RT-PCR product (10 µL) was analysed using 1.5% agarose gel electrophoresis. Generic subunit-specific primers were designed based on mouse subunit sequence information obtained from GenBank (Table 1). Control reactions were carried out in the absence of reverse transcriptase to ensure that the detected products were not the result of possible DNA contamination, and by the use of corresponding templates as positive controls to ensure that the primers annealed successfully. RT-PCR experiments were repeated three times. All amplicons were of the expected sizes and their identities were confirmed by DNA sequence analysis.

HEK293 cell immunofluorescence studies

HEK293 (Dainippon Sumitomo Pharma Co. Ltd., Osaka, Japan) cells were maintained in DMEM (Invitrogen, Tokyo, Japan) supplemented with 10% FBS (Invitrogen, Tokyo, Japan) under a 5% CO_2 atmosphere. Cells were plated on fresh culture dishes every 5–6 days after trypsin treatment. HEK293 cells were transfected with cDNA encoding a green fluorescent protein (GFP) in pcA vector, as well as $K_{IR}6.x$ ($K_{IR}6.1$ or $K_{IR}6.2$) and SUR2B in pECE (Isomoto *et al.*, 1996). Transient transfection was optimized using FuGENE 6 (Roche Applied Science, Indianapolis, IN, USA). Briefly, 80% confluent cultures of HEK293 cells in 35 mm dishes containing acid-washed coverslips (Matsunami Glass Ind., Osaka, Japan) were incubated with cDNAs encoding GFP and K_{ATP} channel subunits and FuGENE 6. Transiently transfected cells were cultured at 37°C and used within 72 h. Transfected HEK293 cells were plated onto glass slides (Matsunami, Osaka, Japan) and incubated at 37°C for 15 min to allow them to adhere to the slides before fixation. Transfected HEK293 cells were fixed in 1–4% paraformaldehyde in PBS for 10–15 min at room temperature, and then washed thoroughly in PBS for

Table 1

Nucleotide sequences for the custom-designed primers used to detect the $K_{IR}6.x$ gene isoforms (*Kcnj8* and *Kcnj11*) and the SUR.x gene isoforms (*Abcc8*, *Abcc9 variant2* and *Abcc9 variant1*) with RT-PCR analysis

Encoding protein name	Gene name	Reference sequence ID	Primer sequence (5′ to 3′)	Size of the amplicons expected (bp)
$K_{IR}6.1$	*Kcnj8*	NM_008428	F- TGCTCTTCGCTATCATGT R- GTTTTCTTGACCACCTGGAT	445
$K_{IR}6.2$	*Kcnj11*	NM_010602	F- TCTGCCTTCCTTTTCTCCAT R- TGCATGTGGATGGTGGCGCT	299
SUR1	*Abcc8*	NM_011510	F- CCCTCTACCAGCACACCAAT R- CAGTCTGCATGAGGCAGGTA	169
SUR2A	*Abcc9 variant2*	NM_021041	F- ATGAAGCCACTGCTTCCATC R- ATCCGTCAAAGTTGGCAAAG	495
SUR2B	*Abcc9 variant1*	NM_011511	F- ATGAAGCCACTGCTTCCATC R- ATCCGTCAAAGTTGGCAAAG	319

10–15 min. The cells were permeabilized in 0.1% polyoxyethylene-p-isooctylphenol (Triton X) in PBS (i.e. 0.1% Triton-X-PBS) for 10–15 min at room temperature. The isolated cells were then washed with PBS (three times for 2 min), and 1% BSA in PBS was applied as a blocking solution for 15 min at room temperature. For $K_{IR}6.x$ staining, dispersed cells were incubated, for 1 h at room temperature, with a rabbit anti-Kir6.1 primary antibody (sc-20808, Santa Cruz Biotechnology, Santa Cruz, CA, USA) or a goat anti-Kir6.2 primary antibody (sc-11228, Santa Cruz Biotechnology), in blocking solution at a 1:200 dilution. Following wash with PBS (three times for 2 min), myocytes were incubated with Alexa Fluor 594 donkey anti-rabbit IgG and Alexa Fluor 488 donkey anti-goat IgG (all 1:200 dilution in blocking solution; Invitrogen, Carlsbad, CA, USA) for 30 min at room temperature, in the dark. The transfected HEK293 cells were then washed with PBS (three times for 2 min), and mounted in Vectashield mounting medium (Vector Laboratories, Burlingame, CA, USA).

Single smooth muscle cell immunofluorescence studies

Single, dissociated myocytes were plated onto glass slides (Matsunami, Osaka, Japan) and incubated at 37°C for 15 min to allow them to adhere to the slides before being fixed. Vas deferens myocytes were fixed in 1–4% paraformaldehyde in PBS for 10–15 min at room temperature, and then washed thoroughly in PBS for 10–15 min. The cells were permeabilized in 0.1% Triton X in PBS (i.e. 0.1% Triton-X-PBS) for 10–15 min at room temperature. The isolated cells were then washed with PBS (three times for 2 min), and 1% BSA in PBS was applied as a blocking solution for 15 min at room temperature. For $K_{IR}6.x$ staining, dispersed cells were incubated, for approximately 1 h at room temperature, with a rabbit anti-$K_{IR}6.1$ primary antibody (sc-20808, Santa Cruz Biotechnology), a goat anti-$K_{IR}6.2$ primary antibody (sc-11228, Santa Cruz Biotechnology) and a mouse monoclonal anti-α-smooth muscle actin primary antibody (Sigma-Aldrich Japan K.K.), diluted in blocking solution at 1:200 dilution. Following wash with PBS (three times for 2 min), myocytes were incubated with Alexa Fluor 594 donkey anti-rabbit IgG, Alexa Fluor 488 donkey anti-goat IgG and Alexa Fluor 647 donkey anti-mouse IgG (all 1:200 dilution in blocking solution; Invitrogen, Carlsbad, CA, USA) for approximately 30 min at room temperature, in the dark. The dispersed smooth muscle cells were then washed with PBS (three times for 2 min) and mounted in Vectashield (Vector Laboratories) mounting medium with DAPI.

Vas deferens myocytes were fixed in 1–4% paraformaldehyde in PBS for 10–15 min at room temperature, and then washed thoroughly in PBS for 10–15 min. The cells were permeabilized in 0.1% Triton X in PBS (i.e. 0.1% Triton-X-PBS) for 10–15 min at room temperature. The isolated cells were then washed with PBS (three times for 2 min), and 1% BSA in PBS was applied as a blocking solution for 15 min at room temperature. For SUR2B staining, dispersed cells were incubated, for approximately 1 h at room temperature, with a goat anti-SUR2B primary antibody (sc-5793, Santa Cruz Biotechnology) and a mouse monoclonal anti-α-smooth muscle actin primary antibody (Sigma-Aldrich Japan K.K), diluted in blocking the solution (1:200 dilution). Following wash with PBS (three times for 2 min), the myocytes were incubated with Alexa Fluor 488 donkey anti-goat IgG and Alexa Fluor 647 donkey anti-mouse IgG (both 1:200 dilution in blocking solution; Invitrogen, Carlsbad, CA, USA) for approximately 30 min at room temperature, in the dark. The dispersed smooth muscle cells were then washed with PBS (three times for 2 min) and mounted in Vectashield mounting medium with DAPI. All the samples were examined using a Nikon A1R confocal microscope system (Nikon, Tokyo, Japan).

Vas deferens myocytes were fixed in 1–4% paraformaldehyde in PBS for 10–15 min at room temperature, and then washed thoroughly in PBS for 10–15 min. The cells were permeabilized in 0.1% Triton X in PBS (*vide supra*) for 10–15 min at room temperature. The isolated cells were then washed with PBS (three times for 2 min), and 1% BSA in PBS was applied as a blocking solution for 15 min at room temperature. As a negative control, the primary antibody was adsorbed with the peptide against which it was made (when available). When not available, it was replaced by the omitted primary antibody. Negative staining controls (not shown) also included a null control, in which the primary antibody was omitted, which tested for non-specific staining of the secondary antibody. To avoid background interference from the secondary antibodies alone, we normally pre-blocked the tissue with 5% normal serum from the same host species as the labelled secondary antibody. We used labelled secondary antibodies that had been pre-adsorbed against mouse and human, and we titrated the labelled secondary antibody to obtain a maximal signal-to-noise ratio.

Immunofluorescence studies

Mouse vasa deferentia were fixed in cold 1% paraformaldehyde for 2 h and washed thoroughly in cold PBS for 2 h. The fixed tissues were embedded in optimal cutting temperature compound (Tissues-Tek, SAKURA, Tokyo, Japan). Tissues in the embedding medium were immediately frozen in liquid nitrogen-cooled hexane. Frozen sections (6 μm thick) were cut with a cryostat (CM3050S, Leica, Tokyo, Japan) and mounted on silane-pre-coated glass slides and allowed to dry in air at room temperature for 30 min. After the sections were washed with PBS (three times for 5 min), the sections were permeabilized in 0.1% saponin in PBS (i.e. 0.1% saponin-PBS) for 30 min at room temperature. The sections were then washed with 0.1% saponin-PBS (three times for 5 min) and blocked with 1% BSA in 0.1% saponin-PBS for 30 min at room temperature. After being washed with 0.1% saponin-PBS (three times for 5 min), sections were incubated with the primary purified rabbit anti-$K_{IR}6.1$ primary antibody (sc-20808, Santa Cruz Biotechnology) diluted (1:200) and a goat anti-SUR2B primary antibody (sc-5793, Santa Cruz Biotechnology) diluted (1:200) in the blocking solution at 4°C overnight in a humidified chamber. Following washing with 0.1% saponin-PBS (three times for 5 min), sections were incubated with Alexa Fluor 594 donkey anti-rabbit IgG and Alexa Fluor 488 donkey anti-goat IgG (Invitrogen, Carlsbad, CA, USA) both diluted to 1:200 in blocking solution for 30 min at room temperature in the dark. Sections were subsequently washed with 0.1% saponin-PBS (three times for 5 min), coverslipped with Vectashield mounting medium with DAPI and examined with a fluorescent microscopy (Biozero BZ-8000,

KEYENCE, Osaka, Japan). Negative staining controls (not shown) also included a null control, in which the primary antibody was omitted, which tested for non-specific staining of the secondary antibody. To avoid background interference from the secondary antibodies alone, the tissue was pre-blocked with 5% normal serum from the same host species as the labelled secondary antibody.

Statistical analysis

Statistical analyses were performed using ANOVA tests (two-factor with replication). Changes were considered significant at $P < 0.05$ (*). Data are expressed as the mean ± SD.

Results

The effects of glibenclamide and U-37883A on pinacidil-induced membrane currents in mouse vas deferens myocytes

Pinacidil was employed to activate whole-cell K_{ATP} currents in dispersed smooth muscle cells isolated from mouse vas deferens, at a holding potential of –70 mV (bath solution, 140 mM K^+ solution; pipette solution, 140 mM KCl solution containing 5 mM EGTA; i.e. symmetrical 140 mM K^+ conditions). Pinacidil caused an inward current in a concentration-dependent manner (30 μM, 303 ± 64 pA, $n = 10$; 100 μM, 915 ± 130 pA, $n = 5$). As shown in Figure 1A, application of pinacidil (100 μM) elicited an inward current that was partially inhibited by 100 nM glibenclamide and completely suppressed by 5 mM Ba^{2+}. Note that Ba^{2+} was utilized to indicate the zero current level at –70 mV. At various time points before and during the application of 100 μM pinacidil (alone or in combination with glibenclamide/Ba^{2+}), six triangular ramp potential pulses (see the inset in Figure 1A) were applied from –120 to 60 mV in order to visualize the current–voltage relationship under each set of experimental conditions (Figure 1A, B). The averaged membrane currents during the falling phases of the ramp pulses under the various experimental conditions are shown in Figure 1B. In Figure 1C, the glibenclamide-sensitive membrane current, obtained by subtracting the averaged membrane current in the presence of both 100 nM glibenclamide and 100 μM pinacidil from that in the presence of pinacidil alone, demonstrated little inward rectification (i.e. the theoretical K^+ equilibrium potential, E_K; 0 mV). Subsequent application of 5 mM Ba^{2+} completely suppressed the pinacidil-induced current.

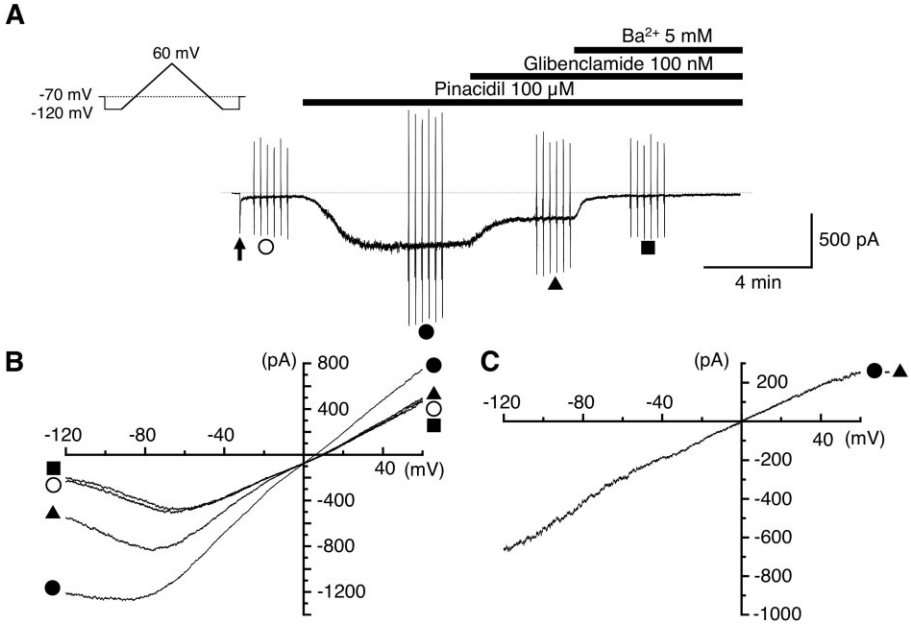

Figure 1

Inhibitory effects of 100 nM glibenclamide and 5 mM Ba^{2+} on the pinacidil-induced membrane current, recorded under symmetrical 140 mM K^+ conditions, in single smooth muscle cells isolated from the mouse vas deferens. A conventional whole-cell configuration was used at a holding potential of –70 mV. The bath solution was PSS containing 140 mM K^+, and the pipette solution contained 140 mM KCl and 5 mM EGTA. (A) Application of pinacidil (100 μM) elicited an inward current at –70 mV. The pinacidil-induced inward current was partially inhibited by glibenclamide (100 nM); the remaining component of the pinacidil-induced current was inhibited by Ba^{2+} (5 mM). The vertical deflections indicate triangular ramp potential pulses (every 15 s; see inset) applied in the absence of any drugs (open circle) or in the presence of 100 μM pinacidil (filled circle), 100 μM pinacidil and 100 nM glibenclamide (filled triangle) or 100 μM pinacidil, 100 nM glibenclamide and 5 mM Ba^{2+} (filled square). The filled arrow indicates the time when a conventional whole-cell configuration was established. The dashed line indicates the zero current level. (B) The mean ramp membrane currents under each experimental condition, shown on an expanded time scale. Symbols as in (A). (C) The glibenclamide-sensitive component of the pinacidil-induced current. Net membrane current was obtained by subtraction of the ramp membrane current recorded in the presence of both 100 μM pinacidil and 100 nM glibenclamide (shown in B, filled triangle) from that recorded in the presence of 100 μM pinacidil alone (shown in B, filled circle).

When voltage ramp pulses were applied and the extracellular K^+ concentration ($[K^+]_o$) was changed by the iso-osmotic substitution of Na^+, the reversal potential of the pinacidil-induced current was obtained in asymmetrical K^+ conditions. Note that the pinacidil-induced current was suppressed by glibenclamide and U-37883A (data not shown). The mean reversal potential of the pinacidil-induced current was –80.1 ± 2.0 mV in 5 mM $[K^+]_o$ (n = 5) and –19.2 ± 2.1 mV in 60 mM $[K^+]_o$ (n = 5; data not shown). These values were close to E_K in each $[K^+]_o$ condition (5 mM $[K^+]_o$, E_K = –84.2 mV; 60 mM $[K^+]_o$, E_K = –21.4 mV). These results suggest that the pinacidil-induced membrane currents are mainly carried by K^+, through K^+ channels, which are sensitive to glibenclamide and U-37883A.

Similar experimental protocols were also performed when U-37883A (10 μM) was applied after the activation of the 100 μM pinacidil-induced current at –70 mV, causing a partial inhibition of the basal amplitude of the current. In the absence of pharmacological blockers (i.e. glibenclamide and U-37883A), the basal amplitude of the pinacidil-induced current at –70 mV gradually decreased after it had reached a maximum value. The rate of decay of the current was determined from measurements made at 30 s intervals, for 8 min, after the peak amplitude had been attained (at 8 min, the amplitude was 0.84 ± 0.08 that of the peak amplitude, n = 8, Figure 2). Thus, in all the experiments where the effects of the selective blockers (glibenclamide or U-37883A) were studied, it was necessary to take into account this decay in the current amplitude. A single concentration of the selective blocker being studied was applied within the 2 min period before the peak amplitude of the pinacidil-induced current was attained. The peak amplitude of the pinacidil-induced current at –70 mV in the absence of any selective blockers was normalized to a value of one, and the amplitude of the inward current measured at 8 min after the application of each concentration of each selective blocker was expressed relative to the peak current in the absence of any blockers. Figure 2 shows concentration-dependent inhibitory curves for the effects of glibenclamide (K_i = 0.3 μM) and U-37883A (K_i = 20.6 μM) on the pinacidil-induced inward currents at –70 mV.

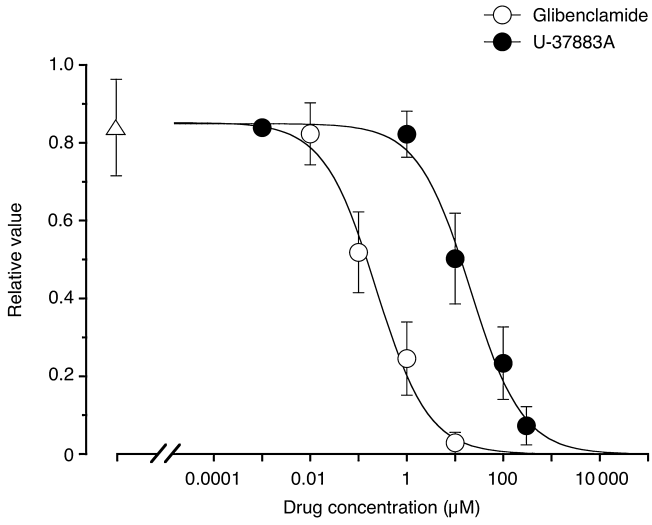

Figure 2

Concentration-response curves for the inhibition of the 100 μM pinacidil-induced current by glibenclamide and U-37883A. The peak amplitude of the pinacidil-induced current at –70 mV in the absence of any selective blockers was normalized to a value of one, measured from the current level in the presence of 5 mM Ba^{2+}, and the amplitude of the inward current measured at 8 min after the application of each concentration of each selective blocker was expressed relative to the peak current in the absence of any blockers. The curves were drawn by fitting with the following equation, using the least-squares method:

$$\text{Relative amplitude} = 1/[1 + (K_i/D)^{nH}]$$

where K_i, D and n_H are the inhibitory dissociation constant, the concentration of each inhibitor (μM) and Hill's coefficient respectively. The following values were used for the curve fitting: glibenclamide, K_i = 0.3 μM, n_H = 0.9; U-37883A, K_i = 20.6 μM, n_H = 0.9.

Sensitivity of the inward current to intracellular ATP in mouse vas deferens myocytes

When ATP was not included in the pipette solution, application of pinacidil (100 μM) caused an inward current (915 ± 130 pA, n = 5, without ATP, Figure 3C). However, when ATP was included in the pipette solution, the peak amplitude of the 100 μM pinacidil-induced current was much smaller (Figure 3A; 3 mM ATP, 10 ± 5 pA, n = 5; 0.3 mM ATP, 126 ± 48 pA, n = 5) than that in the absence of ATP in the pipette solution. When 0.3 mM ATP was included in the pipette solution, the 100 μM pinacidil-induced inward current was suppressed by the additional application of 10 μM glibenclamide (Figure 3A). Figure 3B demonstrates that the cumulative application of MCC-134 (30–100 μM), a SUR modulator, also induced a significant glibenclamide-sensitive inward current, in a concentration-dependent manner. However, application of diazoxide (100 μM) caused no inward current (data not shown). Figure 3C summarizes the relationship between the peak amplitude of the pinacidil-induced inward current and the intracellular ATP level, and also demonstrates that the peak amplitude of the inward current induced by 100 μM MCC-134 was similar to that induced by 100 μM pinacidil (in ATP-free conditions).

Sensitivity of the inward current to intracellular nucleoside diphosphates in mouse vas deferens myocytes

When 3 mM UDP was added to the pipette solution, a significant inward current slowly developed, at a holding potential of –70 mV, after the establishment of a conventional whole-cell configuration (Figure 4A). The UDP-induced inward current reached its maximum amplitude (85 ± 5 pA, n = 5, in 3 mM UDP) in 4–10 min, was sustained for more than 10 min and was sensitive to glibenclamide. It was of interest to examine whether or not other nucleoside diphosphates (NDPs), such as GDP and ADP, could also elicit an inward current. To minimize inter-myocyte variation, we tested each concentration of NDP on cells from the same animal under the same conditions, and the maximum amplitude of the inward current was measured. All three NDPs elicited inward currents that were abolished by glibenclamide (10 μM); this is illustrated for 3 mM UDP and 3 mM GDP in

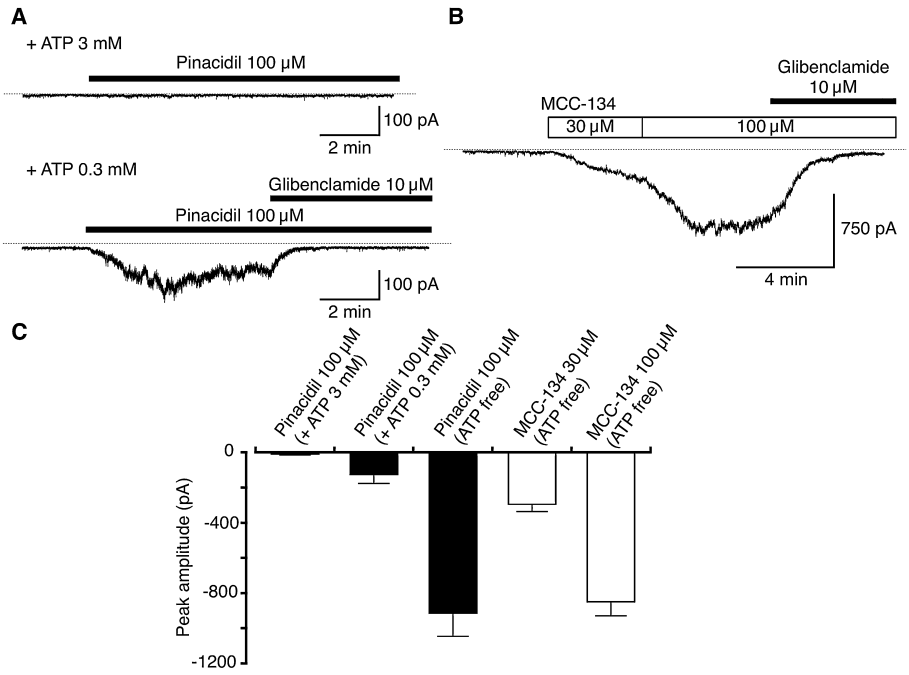

Figure 3

Effects of intracellular ATP concentration on the pinacidil-induced inward current and actions of MCC-134 to elicit an inward current. (A) Inward currents induced by 100 μM pinacidil, recorded (at a holding potential of −70 mV) in the presence of ATP (0.3 and 3 mM) in the pipette solution. The bath solution was PSS containing 140 mM K^+, and the pipette solution contained 140 mM KCl and 5 mM EGTA (i.e. symmetrical 140 mM K^+ conditions). The dashed line indicates the zero current level. (B) Concentration-dependent effects of MCC-134 (30–100 μM) on the membrane current at a holding potential of −70 mV (conventional whole-cell recording). The MCC-134-induced current was suppressed by 5 μM glibenclamide. The dashed line indicates the zero current level. (C) The peak amplitudes of the currents induced by 100 μM pinacidil in the presence of varying ATP concentrations (0, 0.3 and 3 mM) in the pipette solution, and of the currents elicited by the two concentrations of MCC-134 (30 and 100 μM). Columns and bars indicate the mean and SD values respectively. The number of observations at each concentration was 5 or 6.

Figure 4A. The mean data for the peak amplitude of the inward current elicited by each NDP, when included in the pipette solution, is summarized in Figure 4B. The order of potency for the NDPs was UDP > GDP > ADP.

K_{ATP} channel unitary current in single-channel recordings

The cell-attached patch configuration was used to determine the conductances of the pinacidil-induced channel openings. When myocytes were exposed to pinacidil (100 μM) at a holding potential of −70 mV, an increase of approximately 2.6 pA in the K^+ channel-gating current was observed. K_{ATP} channel activity of this amplitude was observed in >95% of the patches tested. To document fully the current–voltage relationship of the unitary currents, voltage steps were applied to potentials between −100 and 60 mV, in increments of 10 mV, in the presence of pinacidil in the bath solution (Figure 5A; $n = 6$). When plotted as shown in Figure 5B, the unitary current–voltage relationship demonstrated a significant departure from linearity at positive potentials, and exhibited a weak but significant inward rectification that was positive to the reversal potential for current flow through the pore (i.e. 0 mV).

Molecular expression of K_{ATP} channel subunits in mouse vas deferens

In order to determine the identity of the subunits potentially contributing to the K_{ATP} channel pores, samples of RNA were isolated from mouse cerebrum and vas deferens, and used in RT-PCR experiments with primers specific for $K_{IR}6.x$ subunits. Specific primers were designed for the amplification of both $K_{IR}6.1$ and $K_{IR}6.2$ mRNAs, to produce cDNA fragments for $K_{IR}6.1$ and $K_{IR}6.2$ respectively (see Table 1). Amplicons were generated from mouse cerebrum RNA samples that were consistent with the products generated using mRNAs encoding $K_{IR}6.1$ and $K_{IR}6.2$ (see Figure 6A). Using the same primers, $K_{IR}6.1$, but not $K_{IR}6.2$, transcripts were detected in vas deferens myocytes.

To identify the subtypes of the modulatory subunits in the K_{ATP} channels, samples of RNA were obtained from mouse ventricular myocytes and vas deferens myocytes. Specific primers were designed for the amplification of SUR.x (SUR1, SUR2A and SUR2B) subunits, to produce cDNA fragments for the genes for these SUR.x isoforms (see Table 1). Positive amplicons for SUR1, SUR2A and SUR2B were detected in cardiac myocytes, while only SUR2B was detected in the vas deferens (Figure 6B). Note that all amplicons were sequenced to confirm their identity.

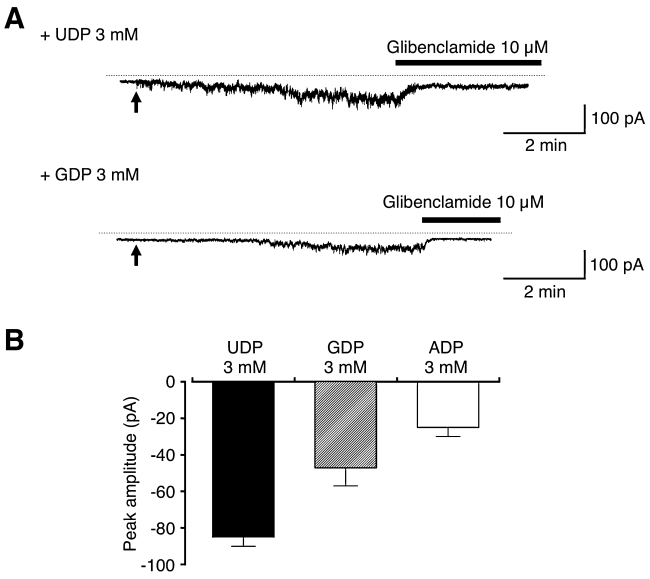

Figure 4

Effects of NDPs (3 mM in the pipette solution) on the membrane current recorded in a conventional whole-cell configuration at –70 mV. (A) Effects of either UDP or GDP (3 mM) on the membrane current. Glibenclamide (10 μM) suppressed the NDP-induced inward currents. The arrows indicate the time when a conventional whole-cell configuration was established. The dashed line indicates the zero current level. (B) The peak amplitude of the NDP-induced current, following inclusion of each NDP in the pipette solution. For each NDP, the current was measured relative to that in the presence of 10 μM glibenclamide. Each column indicates the mean ± SD of six observations.

Immunohistochemical localization of K_{ATP} channel subunits in mouse vas deferens myocytes

In order to identify and localize molecular markers for K_{ATP} channel subunits, immunohistochemical studies were performed. The cross-match test of primary antibodies for $K_{IR}6.x$ ($K_{IR}6.1$ or $K_{IR}6.2$) was performed. When $K_{IR}6.1$ gene was solely transfected with SUR2B gene in HEK293 cells, $K_{IR}6.1$ immunoreactivity, but not $K_{IR}6.2$ immunoreactivity, was clearly visible (Figure 7A–D). When the $K_{IR}6.2$ gene was solely transfected with SUR2B gene in HEK293 cells, $K_{IR}6.2$ immunoreactivity, but not $K_{IR}6.1$ immunoreactivity, was clearly visible (Figure 7E–H). There was no fluorescent reaction of secondary antibodies in the absence of primary antibodies for $K_{IR}6.x$ in HEK293 cells (Figure 7I–L).

In order to identify and localize molecular markers for K_{ATP} channel subunits ($K_{IR}6.x$ and SUR.x), immunohistochemical studies were performed using staining methods for single smooth muscle cells. $K_{IR}6.1$ immunoreactivity was clearly visible in vas deferens myocytes (Figure 8A), while no specific immunoreactive signal was seen for $K_{IR}6.2$ (Figure 8B). Immunoreactivity for α-smooth muscle actin was clearly visible in the smooth muscle cells (data not shown). Since only the SUR2B amplicon was detected in the vas deferens, immunohistochemical methods were employed to confirm the presence of an immunoreactive signal for SUR2B. Immunoreactivity for SUR2B (Figure 9A) was clearly visible in mouse vas deferens myocytes. Immunoreactivity for α-smooth muscle actin was also clearly visible in the smooth muscle cells (data not shown). Using the same antibodies, in order to detect co-localization of $K_{IR}6.1$ and SUR2B proteins in mouse vas deferens, immunohistochemical studies were performed in transverse sections of vas deferens. Both $K_{IR}6.1$ and SUR2B immunoreactivities are clearly visible in the smooth muscle layers of vas deferens (Figure 10).

Discussion

In the present study, we demonstrated that the main molecular composition of mouse vas deferens K_{ATP} channels is likely to be $K_{IR}6.1$/SUR2B.

In freshly dispersed smooth muscle cells isolated from mouse vas deferens, pinacidil (30–100 μM) caused an inward K^+ current in a concentration-dependent manner. Furthermore, it was demonstrated that the 100 μM pinacidil-induced inward currents were suppressed by glibenclamide (K_i = 0.3 μM) and U-37883A (K_i = 20.6 μM) in a concentration-dependent manner. There results strongly suggest the presence of K_{ATP} channels in mouse vas deferens myocytes. Note that Ba^{2+}, an inwardly rectifying K^+ channel blocker, was utilized to obtain the zero current level at –70 mV in order to measure the peak amplitude of the pinacidil-induced inward currents.

Inagaki *et al*. (1995) demonstrated that K_{ATP} channels result from the expression of two different proteins: inwardly rectifying K^+ channel 6.x family pore-forming subunits ($K_{IR}6.x$), and modulatory, SUR.x that are members of the ATP-binding cassette protein superfamily. In general, experiments conducted using the recombinant expression of K_{ATP} channels have provided evidence that $K_{IR}6.2$/SUR1 channels and $K_{IR}6.2$/SUR2A channels represent the predominant isoforms present in pancreatic ß-cells and cardiac myocytes, respectively (Aguilar-Bryan and Bryan, 1999; Seino, 1999). SUR2B associates with $K_{IR}6.2$ (i.e. $K_{IR}6.2$/SUR2B channels) in smooth muscle-type K_{ATP} channels (Isomoto *et al*., 1996). However, in recombinant expression studies, the recombinant channels composed of $K_{IR}6.1$/SUR2B most closely resembled NDP-dependent K^+ channels (i.e. K_{NDP} channels), which have been classified as a subtype of K_{ATP} channel in some vascular smooth muscles (Beech *et al*., 1993). In the present experiments, we demonstrated that each NDP elicited a peak amplitude of the inward current, when included in the pipette solution. Thus, K_{ATP} channels in mouse vas deferens myocytes seem to fall into the category of K_{NDP} channels.

The heterogeneity of the K_{ATP} channels native to smooth muscles is conveyed by various combinations of $K_{IR}6.x$ and SUR.x, as demonstrated by RT-PCR analysis and by the sizes of the unitary conductances measured in single-channel recordings (reviewed by Teramoto, 2006). For instance, $K_{IR}6.2$/SUR2B forms the K_{ATP} channels in murine colon (Koh *et al*., 1998). The expression of transcripts for both K_{ATP} channel pore-forming subunits ($K_{IR}6.1$ and $K_{IR}6.2$) has been detected at the mRNA level in smooth muscle cells, with differences evident between various smooth muscle cell types. For example, K_{ATP} channels have been suggested to

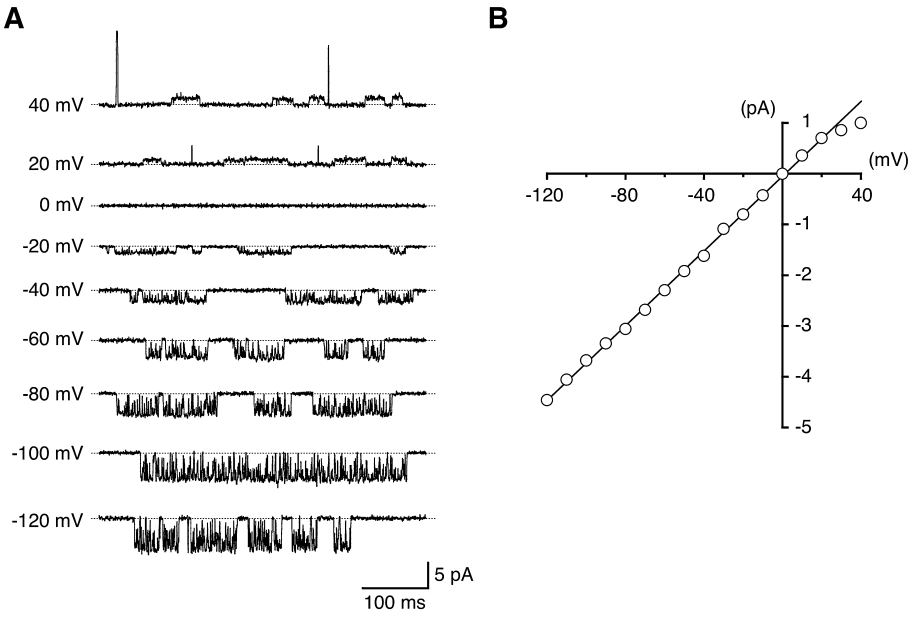

Figure 5

Relationship between the holding membrane potential and the amplitude of the single-channel current activated by 100 μM pinacidil. (A) The traces show channel activities recorded from the same patch at the membrane potentials indicated. The dashed line indicates the current baseline, when the channel was not open. (B) Current–voltage relationship obtained using a cell-attached patch. The amplitudes of the K^+ channel currents were taken from the all-points amplitude histograms for 30 s. The line was fitted by the least-squares method at negative potentials. The channel conductance was 37 ± 1 pS ($n = 6$).

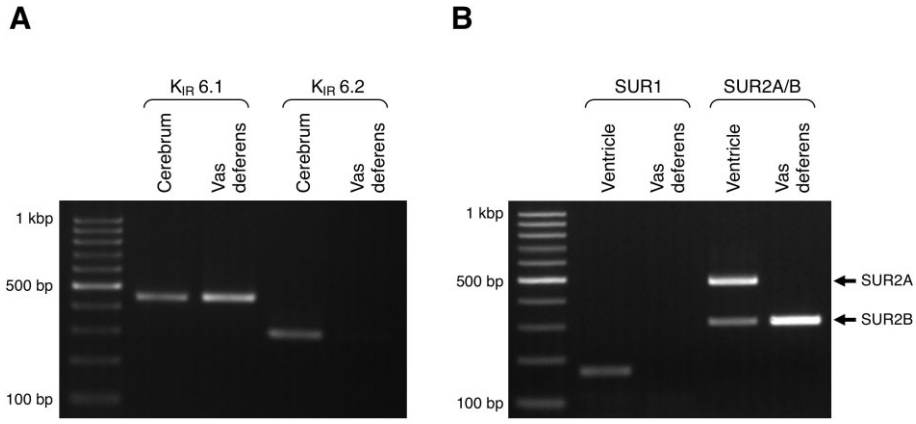

Figure 6

Molecular identification of the K_{ATP} channel subunits by RT-PCR analysis. RT-PCR was performed as described in the Methods, and a ladder was used to indicate the size of the amplified fragments. (A) Specific primers for the K_{IR}6.x gene isoforms (K_{IR}6.1 and K_{IR}6.2) were used, and mRNA was extracted from freshly dissected mouse cerebrum and vas deferens. Amplicons of sizes consistent with those of K_{IR}6.1 (445 bp) and K_{IR}6.2 (299 bp) were evident for the cerebrum, but only K_{IR}6.1 was present in the vas deferens. (B) Specific primers for the SUR.x gene isoforms (SUR1, SUR2A and SUR2B) were used, and mRNA was extracted from freshly dissected mouse ventricle and vas deferens. Amplicons of sizes consistent with those of SUR1 (169 bp), SUR2A (495 bp) and SUR2B (319 bp) were observed in the ventricle, but only SUR2B was evident in the vas deferens.

consist of a homotetrameric structure of K_{IR}6.1 subunits in gastric myocytes (Sim *et al.*, 2002), to be a heteromultimerization of K_{IR}6.1 and K_{IR}6.2 subunits in pig urethra (Teramoto *et al.*, 2009), and to have multiple homotetrameric structural pore regions in vascular smooth muscle (rat portal vein; Zhang and Bolton, 1996; Cole *et al.*, 2000). The use of additional experimental techniques will help in the elucidation of the molecular properties of the channel pore subunits found in the various native smooth muscle cell-type K_{ATP} channels. New technical approaches could include the utilization of specific pharmacological tools (such as K_{ATP} channel blockers or K_{ATP} channel openers) against K_{ATP} channels, and immuno-

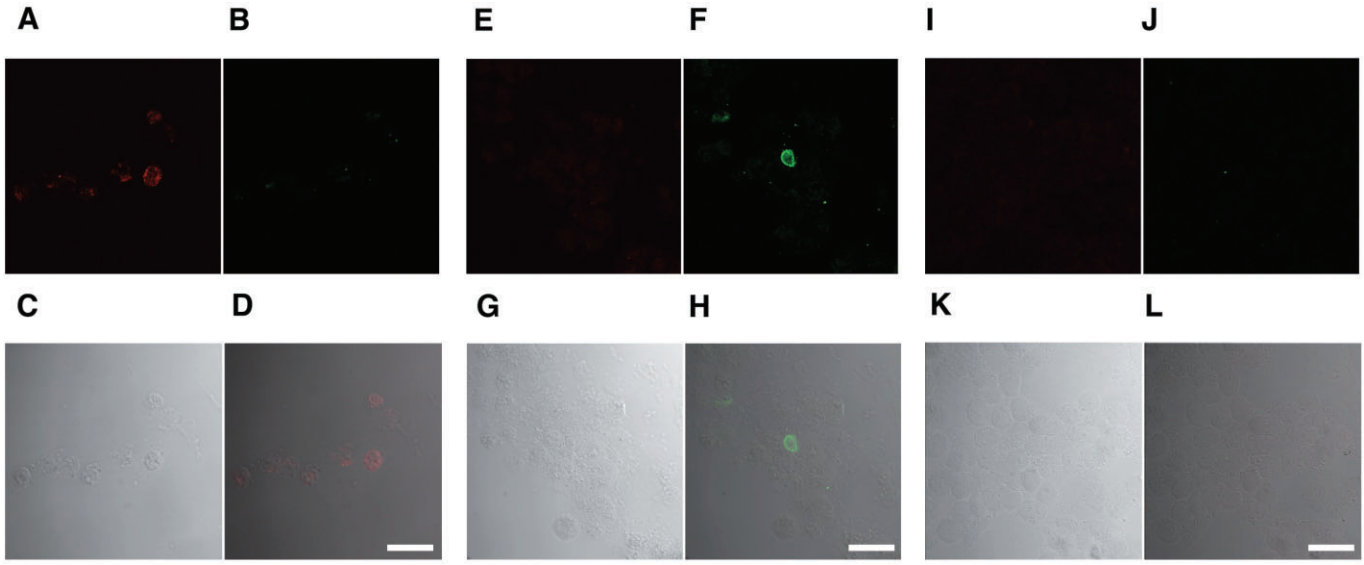

Figure 7

The cross-match test of primary antibodies for $K_{IR}6.x$ ($K_{IR}6.1$ or $K_{IR}6.2$) transfected with the SUR2B gene in HEK293 cells. White bar represents 20 μm. (A–D) When the $K_{IR}6.1$ gene was solely transfected with the SUR2B gene in HEK293 cells, $K_{IR}6.1$ immunoreactivity (A), but not $K_{IR}6.2$ immunoreactivity (B), was clearly visible in HEK293 cells. Transmission image (C). (D) is an overlay of panels A, B and C. (E–H) When the $K_{IR}6.2$ gene was solely transfected with the SUR2B gene in HEK293 cells, $K_{IR}6.2$ immunoreactivity (F), but not $K_{IR}6.1$ immunoreactivity (E), was clearly visible in HEK293 cells. Transmission image (G). (H) is an overlay of panels E, F and G. (I–L) No fluorescent reaction of second antibodies in the absence of primary antibodies (Alexa Fluor 594 donkey anti-rabbit IgG (I); Alexa Fluor 488 donkey anti-goat IgG (J)) in HEK293 cells. Transmission image (K). (L) is an overlay of panels I, J and K.

histochemical analyses of $K_{IR}.6.x$ and SUR.x subunits although there are some limitations with these techniques. However, such approaches could be combined with electrophysiology to measure the size of the channel conductance, as well as with RT-PCR to detect mRNA expression.

In the present experiments, the $K_{IR}6.x$ subtype of the channel in mouse vas deferens myocytes displayed the following characteristics: (i) the conductance was ~37 pS in cell-attached and excised patches, which is similar to that of $K_{IR}6.1$. (ii) The current showed weak inward rectification at positive membrane potentials. (iii) U-37883A, a selective $K_{IR}6.1$ blocker (Kovalev *et al.*, 2004), suppressed the K_{ATP} current. (iv) A transcript of *Kcnj8* (the $K_{IR}6.1$ gene), but not *Kcnj11* (the $K_{IR}6.2$ gene), was detected by RT-PCR analysis. (v) Using immunohistochemical techniques, $K_{IR}6.1$ protein, but not $K_{IR}6.2$ protein, was detected in single smooth muscle cells isolated from mouse vas deferens. Based on these observations, it is most likely that the mouse vas deferens K_{ATP} channel pore is composed of $K_{IR}6.1$ subunits.

The molecular properties of SUR.x in mouse vas deferens K_{ATP} channels were as follows: (i) RT-PCR analysis: three different types of SUR.x (i.e. SUR1, SUR2A and SUR2B) gene were detected in mouse ventricle at all developmental times (adult, neonatal and fetal stages, Morrissey *et al.*, 2005a). Recent immunohistochemical studies have also detected not only SUR2A, but also SUR1 and SUR2B proteins in ventricular myocytes (SUR1, Morrissey *et al.*, 2005b; SUR2B, Zhou *et al.*, 2007). Thus, in RT-PCR analysis, it seems that the ventricular myocyte is likely to be a useful positive control cells to detect three different types of SUR.x. In the current study, we also clearly showed the presence of three different types of SUR.x (i.e. SUR1, SUR2A and SUR2B) gene in mouse ventricular myocytes. Thus, it is probable that three different types of SUR.x (i.e. SUR1, SUR2A and SUR2B) subunit may be present in cardiac myocytes at the mRNA and protein levels. In the present experiments, it was ensured that each primer was able to detect the individual gene of each SUR.x as a positive control. Under these experimental conditions, only transcripts of the SUR2B gene, but not transcripts of the SUR2A gene, were detected at the mRNA level in mouse vas deferens myocytes, despite the use of the same set of primers; transcripts of the SUR1 genes were also not detected. (ii) MCC-134 induced activity: it has been reported that MCC-134 is a useful pharmacological agent with which to identify the SUR.x subtype (Shindo *et al.*, 2000). It is believed that MCC-134 acts as an inverse agonist at SUR1, a partial agonist at SUR2A and a full agonist at SUR2B, and hence its effects depend on the type of SUR.x in the K_{ATP} channels (Shindo *et al.*, 2000). In the present experiments, MCC-134 elicited K_{ATP} currents in mouse vas deferens, but it is noteworthy that the activity induced by 100 μM MCC-134 was similar to that induced by 100 μM pinacidil. Similar results were reported in HEK293 cell expression studies, demonstrating that MCC-134 possesses almost the same potency and efficacy as pinacidil in activating SUR2B/$K_{IR}6.2$ channels but is much less effective than pinacidil in activating SUR2A/$K_{IR}6.2$ channels (Shindo *et al.*, 2000). (iii) Anti-SUR2B immunoreactivity: anti-SUR2B immunoreactivity was clearly visible in single cardiac myocytes (mouse, Morrissey *et al.*, 2005a; rat, Morrissey *et al.*, 2005b) and human detrusor (Aishima *et al.*, 2006). Using the same anti-SUR2B primary antibody, anti-SUR2B immunoreactivity was clearly detected in single smooth muscle cells

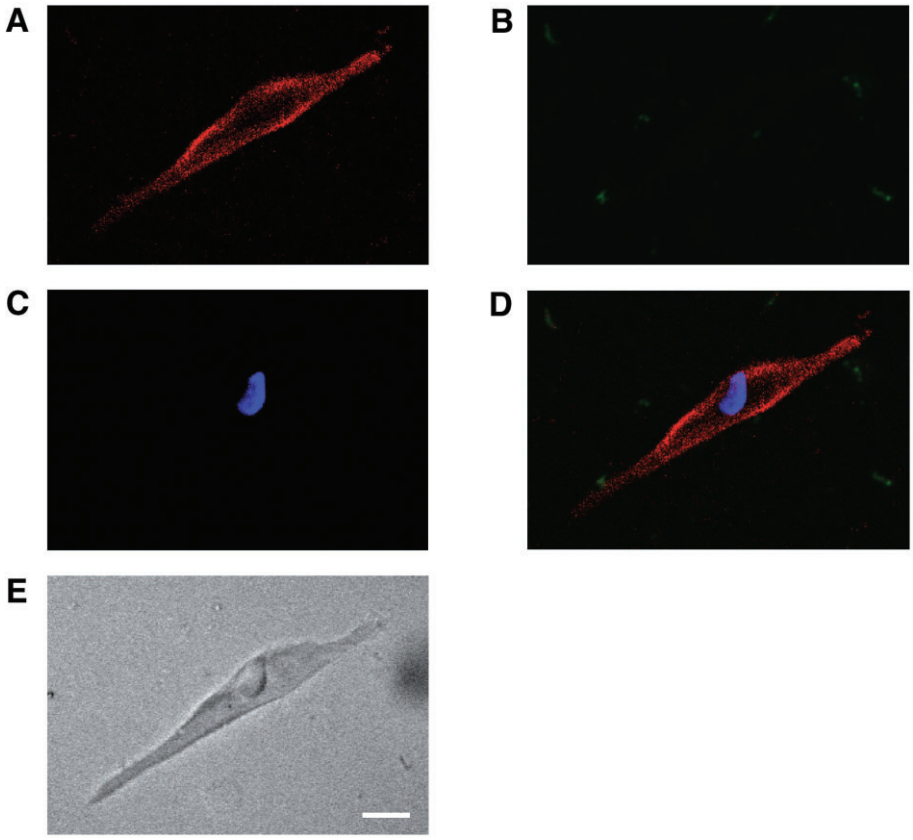

Figure 8

Immunohistochemical localization of $K_{IR}6.1$ and $K_{IR}6.2$ subunits in myocytes isolated from the mouse vas deferens. (A) Immunoreactivity of the anti-$K_{IR}6.1$ antibody. (B) Immunoreactivity of the anti-$K_{IR}6.2$ antibody. (C) DAPI nucleic acid stain. (D) An overlay of panels A, B and C. (E) Transmission image of the mouse vas deferens myocyte. White bar in (E) represents 100 μm.

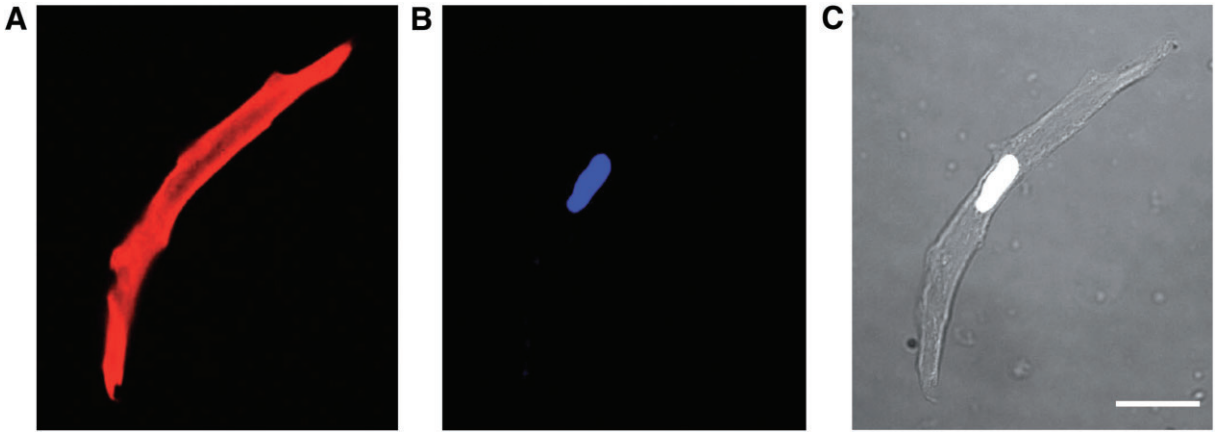

Figure 9

Immunohistochemical localization of SUR2B subunits in mouse vas deferens myocytes. (A) Immunoreactivity of the anti-SUR2B antibody. (B) DAPI nucleic acid stain. (C) Transmission image of the mouse vas deferens myocyte. White bar in (C) represents 100 μm.

dispersed from mouse vas deferens. Based on these observations (RT-PCR analysis, effects of MCC-134 on the membrane currents and anti-SUR2B immunoreactivity), it is most likely that the major SUR.x modulatory subunit in mouse vas deferens is SUR2B.

Taken together, these results indicate that $K_{IR}6.1$ is almost certainly the main subunit of the channel pore protein, and SUR2B is probably the major modulatory SUR subunit in mouse vas deferens myocytes. Thus, our findings indicate that the molecular composition of the K_{ATP} channel in mouse

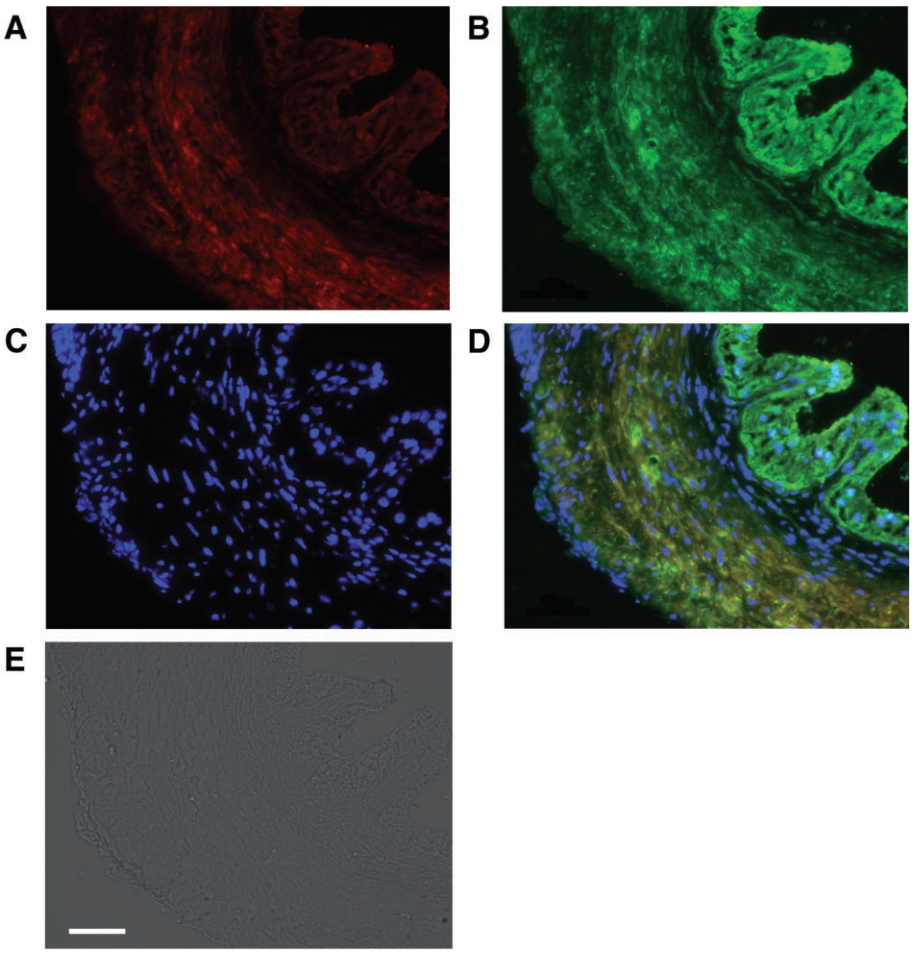

Figure 10

Images of transverse sections of vas deferens showing fluorescent labelling of immunoreactivity for $K_{IR}6.1$ and SUR2B. (A) Immunoreactivity detected with anti-$K_{IR}6.1$ antibody. (B) Immunoreactivity of the anti-SUR2B antibody. (C) DAPI nucleic acid stain. (D) An overlay of panels A, B and C. (E) Structure revealed with Nomarski differential interference contrast imaging. Bar (white line) in (E) represents 50 μm.

vas deferens myocytes appears to be that of a $K_{IR}6.1$/SUR2B complex, which is similar to the K_{NDP} channel subtype found in vascular smooth muscle (Teramoto, 2006).

In conclusion, this study provides novel evidence that native K_{ATP} channels in mouse vas deferens myocytes are a heterocomplex of $K_{IR}6.1$ channels and SUR2B subunits.

Acknowledgements

This work was supported by a Funding Program for Next Generation World-Leading Researchers (Noriyoshi Teramoto, Grant Number LS096) from the Japanese Society for the Promotion of Science.

Conflict of interest

The authors declare no conflicts of interest, financial or otherwise.

References

Aguilar-Bryan L, Bryan J (1999). Molecular biology of adenosine triphosphate-sensitive potassium channels. Endocr Rev 20: 101–135.

Aishima M, Tomoda T, Yunoki T, Nakano T, Seki N, Yonemitsu Y *et al.* (2006). Actions of ZD0947, a novel ATP-sensitive K^+ channel opener, on membrane currents in human detrusor myocytes. Br J Pharmacol 149: 542–550.

Alexander SPH *et al.* (2013). The Concise Guide to PHARMACOLOGY 2013/14: Overview. Br J Pharmacol 170: 1449–1867.

Beech DJ, Zhang H, Nakao K, Bolton TB (1993). K channel activation by nucleotide diphosphates and its inhibition by glibenclamide in vascular smooth muscle cells. Br J Pharmacol 110: 573–582.

Cole WC, Malcolm T, Walsh MP, Light PE (2000). Inhibition by protein kinase C of the K_{NDP} subtype of vascular smooth muscle ATP-sensitive potassium channel. Circ Res 87: 112–117.

Eltze M (1989). Competitive antagonism by glibenclamide of cromakalim inhibition of twitch contractions in rabbit vas deferens. Eur J Pharmacol 161: 103–106.

Grana E, Boselli C, Bianchi L (1997). Cromakalim blocks the purinergic response evoked in rat vas deferens by single-pulse electrical stimulation. Eur J Pharmacol 319: 57–64.

Harhun MI, Jurkiewicz A, Jurkiewicz NH, Kryshtal DO, Shuba MF, Vladimirova IA (2003). Voltage-gated potassium currents in rat vas deferens smooth muscle cells. Pflügers Arch 446: 380–386.

Inagaki N, Gonoi T, Clement JP IV, Namba N, Inazawa J, Gonzalez G *et al*. (1995). Reconstitution of IK_{ATP}: an inward rectifier subunit plus the sulfonylurea receptor. Science 270: 1166–1170.

Isomoto S, Kondo C, Yamada M, Matsumoto S, Higashiguchi O, Horio Y *et al*. (1996). A novel sulfonylurea receptor forms with BIR (Kir6.2) a smooth muscle type ATP-sensitive K^+ channel. J Biol Chem 271: 24321–24324.

Kato K, Furuya K, Tsutsui I, Ozaki T, Yamagishi S (2000). Cyclic AMP-mediated inhibition of noradrenaline-induced contraction and Ca^{2+} influx in guinea-pig vas deferens. Exp Physiol 85: 387–398.

Kilkenny C, Browne W, Cuthill IC, Emerson M, Altman DG (2010). Animal research: Reporting *in vivo* experiments: The ARRIVE guidelines. Br J Pharmacol 160: 1577–1579.

Koh SD, Bradley KK, Rae MG, Keef KD, Horowitz B, Sanders KM (1998). Basal activation of ATP-sensitive potassium channels in murine colonic smooth muscle cell. Biophys J 75: 1793–1800.

Kovalev H, Quayle JM, Kamishima T, Lodwick D (2004). Molecular analysis of the subtype-selective inhibition of cloned K_{ATP} channels by PNU-37883A. Br J Pharmacol 141: 867–873.

McGrath J, Drummond G, McLachlan E, Kilkenny C, Wainwright C (2010). Guidelines for reporting experiments involving animals: the ARRIVE guidelines. Br J Pharmacol 160: 1573–1576.

Morrissey A, Parachuru L, Leung M, Lopez G, Nakamura TY, Tong X *et al*. (2005a). Expression of ATP-sensitive K^+ channel subunits during perinatal maturation in the mouse heart. Pediatr Res 58: 185–192.

Morrissey A, Rosner E, Lanning J, Parachuru L, Dhar Chowdhury P, Han S *et al*. (2005b). Immunolocalization of K_{ATP} channel subunits in mouse and rat cardiac myocytes and the coronary vasculature. BMC Physiol 5: 1–18.

Patel AI, Hennan JK, Diamond J (1997). Activation of guanosine 3′,5′-cyclic monophosphate (cGMP)-dependent protein kinase in rat vas deferens and distal colon is not accompanied by inhibition of contraction. J Pharmacol Exp Ther 283: 894–900.

Seino S (1999). ATP-sensitive potassium channels: a model of heteromultimeric potassium channel/receptor assemblies. Annu Rev Physiol 61: 337–362.

Shindo T, Katayama Y, Horio Y, Kurachi Y (2000). MCC-134, a novel vascular relaxing agent, is an inverse agonist for the pancreatic-type ATP-sensitive K^+ channel. J Pharmacol Exp Ther 292: 131–135.

Sim JH, Yang DK, Kim YC, Park SJ, Kang TM, So I *et al*. (2002). ATP-sensitive K^+ channels composed of Kir6.1 and SUR2B subunits in guinea pig gastric myocytes. Am J Physiol 282: G137–G144.

Soares-da-Silva P, Fernandes MH (1990). Inhibition by the putative potassium channel opener pinacidil of the electrically-evoked release of endogenous dopamine and noradrenaline in the rat vas deferens. Naunyn Schmiedebergs Arch Pharmacol 342: 415–421.

Teramoto N (2006). Physiological roles of ATP-sensitive K^+ channels in smooth muscle. J Physiol 572: 617–624.

Teramoto N, Brading AF (1996). Activation by levcromakalim and metabolic inhibition of glibenclamide-sensitive K channels in smooth muscle cells of pig proximal urethra. Br J Pharmacol 118: 635–642.

Teramoto N, Zhu HL, Shibata A, Aishima M, Walsh EJ, Nagao M *et al*. (2009). ATP-sensitive K^+ channels of pig urethral smooth muscle cells are heteromultimers of Kir6.1 and Kir6.2. Am J Physiol 296: F107–F117.

Wassall RD, Teramoto N, Cunnane TC (2009). Noradrenaline: a remarkable and still elusive neurotransmitter. In: Squire LE (ed.). The New Encyclopedia of Neuroscience. Elsevier Ltd.: New York, pp. 1221–1230.

Zhang H-L, Bolton T (1996). Two types of ATP-sensitive potassium channels in rat portal vein smooth muscle cells. Br J Pharmacol 118: 105–114.

Zhou M, He H-J, Suzuki R, Liu K-X, Tanaka O, Sekiguchi M *et al*. (2007). Localization of sulfonylurea receptor subunits, SUR2A and SUR2B, in rat heart. J Histochem Cytochem 55: 795–804.

Zhu HL, Aishima M, Morinaga H, Wassall RD, Shibata A, Iwasa K *et al*. (2008). Molecular and biophysical properties of voltage-gated Na^+ channels in murine vas deferens. Biophys J 94: 3340–3351.